ISSN 1063-7842, Technical Physics, 2015, Vol. 60, No. 3, pp. 451–455. © Pleiades Publishing, Ltd., 2015.
Original Russian Text © M.M. Kasumov, O.I. V'yunov, 2015, published in Zhurnal Tekhnicheskoi Fiziki, 2015, Vol. 85, No. 3, pp. 133–137.

EXPERIMENTAL INSTRUMENTS AND TECHNIQUE

Mass Spectrometry Determination of the Properties of the Fullerite Consisting of a C_{60}–C_{70} Mixture

M. M. Kasumov* and O. I. V'yunov**

Vernadsky Institute of General and Inorganic Chemistry, National Academy of Sciences of Ukraine, pr. Palladina 32/34, Kyiv, 03680 Ukraine
**e-mail: kasumova@meta.ua*
***e-mail: vyunov@ionic.kiev.ua*

Received January 22, 2014; in final form, July 21, 2014

Abstract—The transformations of the crystal structure of the fullerite consisting of a mixture of C_{60} and C_{70} that occur in the course of heating during pulsed laser irradiation are described using experimental results, the fullerite surface temperature is determined during secondary synthesis, and the absorption coefficient of laser radiation is calculated.

DOI: 10.1134/S106378421503010X

1. INTRODUCTION

The discovery of fullerenes and their derivatives, which have unique properties, and the development of the arc method of their synthesis have been a powerful stimulus to searching for and improving synthesis and analysis methods and to developing application methods for more than two decades. An obvious advantage of this material is the availability of initial raw materials and the simplicity of the synthesis method.

The first applications of the new material were based on the properties of fullerenes as carbon clusters, which have a high electron affinity unlike other materials. This property of fullerenes is used in solar batteries, and high parameters of these batteries are reached if heavy C_i ($i > 70$) fullerenes are employed as an electron acceptor due to a large cross section and a high electron affinity [1]. This specific feature determined the nucleation of a new branch of physics, chemistry, and the technology of production and application of fullerenes. Among the number of other applications, we note the use of fullerenes for the growth of diamond films. The wear resistance of moving machine parts and mechanisms increases significantly when they are coated with diamond films made of fullerenes.

The recently developed method of synthesizing a hydrolyzed structure of C_{60} fullerene, namely, fullerenol-d, favors a wide use of fullerene structures in various fields of science, engineering, industry, and medicine [2]. Structures with a conventional mass of 1128 Da and conventional formula $C_{60}(OH)_{24}$ are used in aqueous and salt solutions and the solutions related to the vital activity of the human being. Therefore, it is necessary to supplement the concepts of these structures and their transformations, which can be done with new analysis methods.

At present, information on the properties of fullerenes become available when surface- or matrix-assisted laser desorption ionization-time of flight (SALDI-TOF or MALDI-TOF) laser mass spectrometry (MS) is used. These methods are applied to study the multiatomic components in complex structures, and they are based on time-of-flight analysis of the structures evaporated/ionized during the action of a pulsed laser beam [3]. In this work, we perform the SALDI-TOF MS method using an AutoFlex mass spectrometer. To study the volume properties of the mixture fullerite, we delayed the formation of an ion flux with respect to the pulsed laser beam used for evaporation.

Based on the mass spectra of the fullerite and the thermophysical parameters, we describe the transformations of fullerite crystallites in heating under the action of a pulsed laser beam and estimate the fullerite temperature during secondary synthesis. We were the first to estimate the absorption coefficient of the N_2 laser radiation using experimental and reported data.

2. LASER MASS SPECTROMETRY STUDY OF THE STRUCTURAL TRANSFORMATIONS IN THE MIXTURE FULLERITE

In Section 2, we analyze the transformations that occur on the fullerite surface by recording the mass spectrum of negatively charged fullerenes under the action of a laser beam with the optimum radiation power density. We study the mass spectrum of a sample of the fullerenes synthesized at an arc current of 100 A, a helium flow rate $q = 2$ cm^3/s, and a pressure $p \approx 0.11$ MPa. The fullerenes were extracted from soot in benzene and fullerene samples were prepared on an Al substrate. Mass spectra were recorded on an AutoFlex

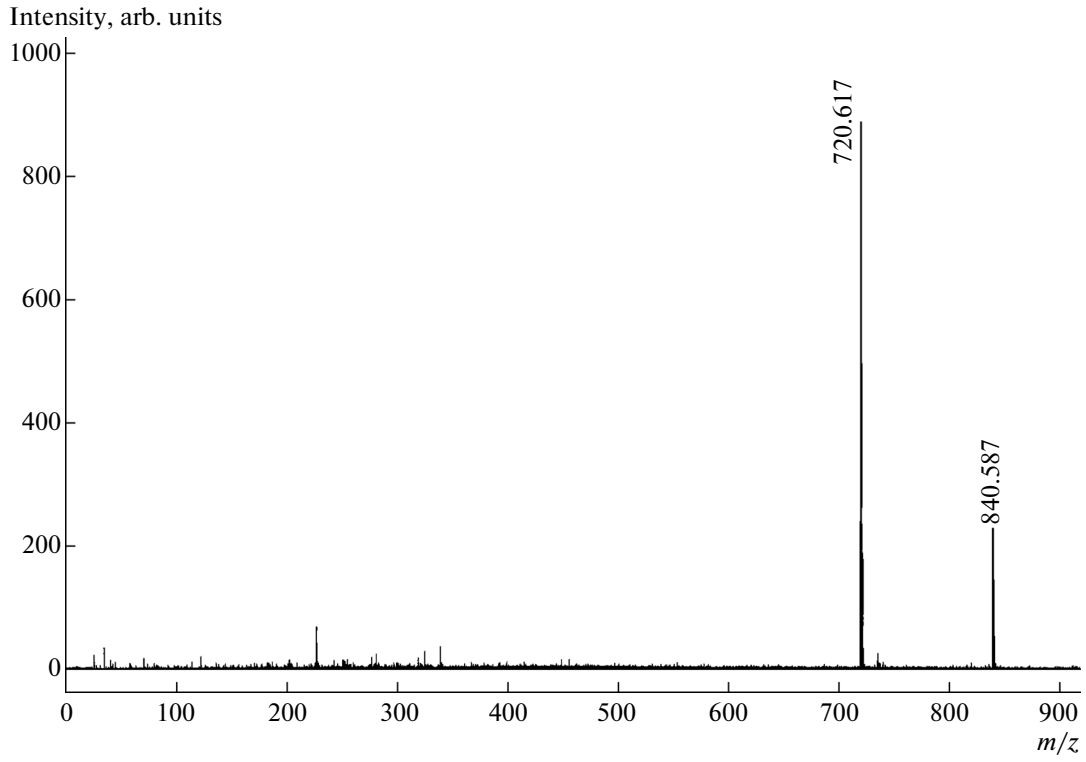

Fig. 1. Mass spectrum of negatively charged ions at $W = 0.12$ MW/cm^2.

(Bruker, Germany) time-of-flight mass spectrometer equipped with a N_2 laser ($\lambda = 337$ nm) at a laser pulse duration $\tau_0 = 3$ ns.

The optimum laser beam power for the formation of a mass spectrum of fullerenes was experimentally chosen in order to achieve sufficiently high peaks of the main spectrum components relative to the background. An example of such a mass spectrum is shown in Fig. 1.

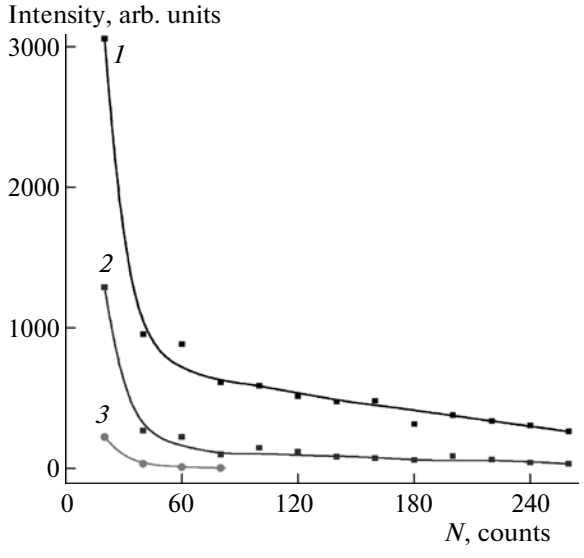

Fig. 2. Peaks of fullerenes (*1*) C_{60}^-, (*2*) C_{70}^-, and (*3*) $C_{60}O^-$ vs. the number of laser pulses N. The radiation pulse energy is $q = 3.5$ μJ, $f = 5$ s^{-1}, and the extracting voltage delay is $\tau^* = 30$ ns.

It is seen from Fig. 1 that background structures have a level of 1–5% of the peak of C_{60} under these conditions. Therefore, the optimum laser radiation power density for the mixture fullerite was taken to be $W_0 \approx 0.1$ MW/cm^2. To determine the fullerite surface temperature, we used the formula from [4]. It shows that the fullerite surface temperature during the sublimation of the fullerite consisting of a mixture of C_{60} and C_{70} is

$$T = 1032/[0.35 + \log(I_{60}/I_{70})], \quad (1)$$

where I_{60}/I_{70} is the ratio of the peaks of C_{60} to C_{70} in the mass spectrum.

The calculation of the mass spectrum shown in Fig. by Eq. (1) demonstrates that the sample surface temperature is $T \approx 1045$ K, which is significantly higher than the fullerene dimerization temperature [5, 6].

Figure 2 shows the peaks of C_{60}, C_{70}, and $C_{60}O$ nanostructures from the 13 mass spectra recorded from the same point in a fullerite sample at $W = 0.12$ MW/cm^2.

As is seen from Fig. 2, curves *1–3* have similar shapes: the line peaks decrease with increasing number of laser pulses. Curves *1* and *2* can be divided into two sections in the slope. The initial steepest section in

curves *1* and *2* in Fig. 2 corresponds to desorption with the minimum energy threshold. The degradation of fullerite crystallites is the process that requires the minimum energy. For C_{60} and C_{70}, the enthalpy of crystallite sublimation is $q_1 = 1.88\ (1 \pm 0.02)$ eV and $q_2 = 2.0\ (1 \pm 0.02)$ eV, respectively [7–10]. In other words, the degradation of crystalline structures in the initial section is accompanied by intense desorption of fullerenes, since the sample crystallites formed on the substrate when the solvent was removed under the action of relatively weak van der Waals forces. During the degradation of the crystallites, the evaporation intensity decreases and the second gentle section in curves *1* and *2* in Fig. 2 starts. In this section, the evaporation intensity is determined by the process having the maximum threshold and fullerenes degrade. The energy of atomization of fullerenes C_{60} and C_{70} is $q_1^* = 7.4$ eV and $q_2^* = 8.1$ eV, respectively [7–10]. It is interesting that, after mass-spectrometric measurements, the laser-beam-treated area in the sample becomes dark brown and a thin soot layer is visible. These features demonstrate that, under the action of a laser beam at $W \approx 0.1$ MW/cm^2 during mass-spectrometric analysis, fullerenes undergo a phase transition into a stable phase, namely, amorphous component (graphite) [6, 8–12]. This material has a high evaporation temperature and accumulates on the fullerite surface. Fullerene fragments screen laser radiation and, thus, decrease the effective sample surface. As a result, the peak intensities decrease and the gentle section in curves *1* and *2* in Fig. 2 forms.

Curve *3* in Fig. 2 differs from curves *1* and *2* and exhibits a significant drop after the first series of laser pulses. This specific feature demonstrates that the $C_{60}O$ oxide forms on the crystallite surface and does not form on its fragments during the degradation of crystallites.

To estimate the process quantitatively, we performed a calculation using curves *1* and *2* in Fig. 2. The experimental slope of the curve for cluster C_n was determined from the ratio $F_n = \Delta A_n/\Delta t_n$, where $\Delta A_n/$ is the change of the peak of the cluster in time interval $\Delta t_n = \kappa \times \Delta N_n$. Here, κ is a coefficient and ΔN_n is the number of pulses in time interval Δt_n. The ratio of the slopes in the first and second sections is $M_n = F_{n1}/F_{n2}$, where F_{n1} and F_{n2} are the slopes of the first and second sections, respectively. The experimental relative decreases of the slopes in Fig. 2 are as follows:

curve *1* for fullerene C_{60}, $M_{60} = F_{60.1}/F_{60.2} = 37$; (2)

curve *2* for fullerene C_{70}, $M_{70} = F_{70.1}/F_{70.2} = 51$. (3)

On the other hand, these parameters can be obtained from the ratio of the threshold values of these structures. Indeed, for fullerite C_{60} we have

$$q_1^*/q_1 = 3.94, \quad (2^*)$$

for fullerite C_{70},

$$q_2^*/q_2 = 4.05. \quad (3^*)$$

Thus, the slopes of curves *1* and *2* calculated by Eqs. (2) and (3), respectively, using the experimental data in Fig. 2 agree with the ratios of the thresholds of degradation of crystallite/cluster structures that are calculated by Eqs. (2*) and (3*), respectively.

3. OPTICAL PROPERTIES OF THE MIXTURE FULLERITE. DETERMINATION OF THE ABSORPTION COEFFICIENT OF LASER RADIATION

In Section 3, we measure the mass spectrum of positively and negatively charged fullerene ions using a laser beam at a radiation power density $W = 0.33$ MW/cm^2, which is sufficient for secondary synthesis and studying the optical properties of the fullerite (which are unknown) [13].

The mass spectra of fullerenes were recorded as a function of the delay of the extracting voltage, which was determined as $\tau = 10v$ ns, were $v = 1, 2, \ldots, 5$ with respect to the end of the laser pulse forming the spectrum. The last mass spectrum is shown in Fig. 3.

The mass spectrum in Fig. 3 consists of two different sections. The first section includes the peaks of initial structures C_{60}^- ($m/z = 720.149$) and C_{70}^- (840.033) and the lines of oxides $C_{60}O^-$ and $C_{70}O^-$ the peaks of which account for 15% of the peaks of the initial structures. Moreover, the line of fullerene C_{84} (1008.242) accounts for 7% of the level of the line of C_{60}. The second section in the mass spectrum in Fig. 3 consists of the closely spaced peaks of the secondary synthesis particles. It is seen that some peaks of secondary synthesis are comparable with the peaks of the initial structures and the lines of the structures are spaced $\Delta(m/z) = 12u$ apart. The lines of hydrated carbon isotopes are located between the principal lines in the spectrum [13]. The spectrum in Fig. 3 is characterized by the alternation of peaks with even and odd numbers of carbon atoms, and the peaks with an even number of carbon atoms are lower than those with an odd number of carbon atoms by a factor of 1.5–3. For example, the spectrum in Fig. 3 has the lines of C_{19}^- (227.624), C_{20}^- (240.618), and C_{21}^- (251.625). Among these structures, C_{21} is largest and C_{20} is smallest. By definition, an even number of carbon atoms is a sign of a closed structure, i.e., fullerene; for a fullerene, the number of bonds $N = 3n/2$ is an integer if n is an even number.

In Fig. 4, we show the peak intensities of C_{60} (curve *1*) and C_{70} (curve *2*) as functions of delay time τ with respect to a laser pulse among the five mass spectra of negatively charged fullerenes.

Curves *1* and *2* are similar and have a domelike shape. Using the data in Fig. 4 and Eq. (1), we calculated the fullerite surface temperature, and the calculation results are illustrated by curve *3*. It is seen that

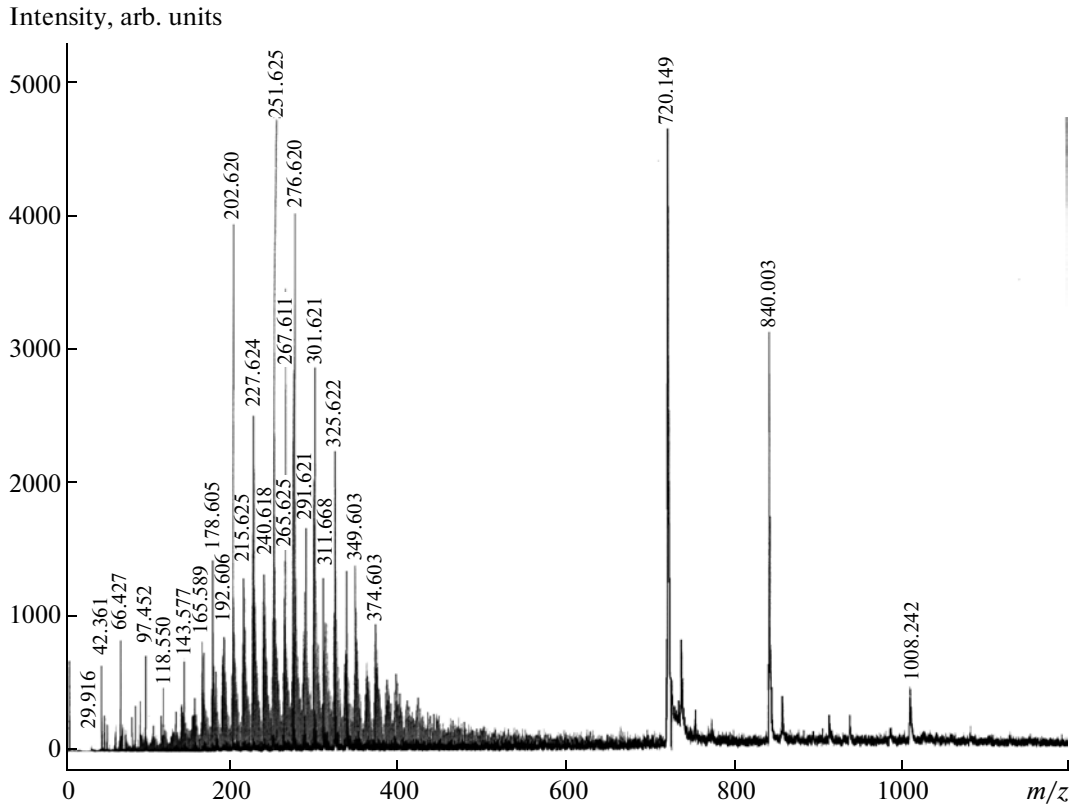

Fig. 3. Mass spectrum of negatively charged fullerite ions that was recorded at a delay $\tau = 50$ ns with respect to a laser pulse.

the initial point in curves *1–3* is time $\tau_1 = 20$ ns after which a plateau 10–20 ns long is observed in the curves. The curves in Fig. 4 are explained by the model concept of surface evaporation [14]: a sublimation flux starts from a surface fullerite layer several interatomic distances thick. Heat energy from an absorption layer L (to be determined later) to an evaporation layer is transferred due to the heat conduction of fullerite. The fullerite surface temperature increases from $T_1 = 1950$ K,

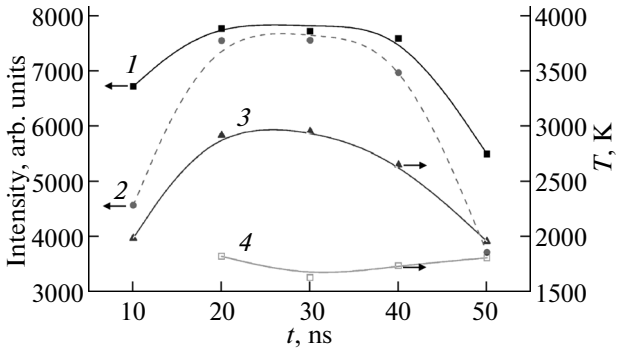

Fig. 4. Peaks of fullerenes (*1*) C_{60}^- and (*2*) C_{70}^-, (*3*) fullerite temperature during the formation of negatively charged fullerene ions, and (*4*) fullerite temperature during the formation of positively charged fullerene ions vs. extracting voltage delay time τ.

and the maximum temperature of the fullerite surface $T_{max} = 2950$ K is reached in a time $20 \le \tau_i < 30$ ns (Fig. 4, curve *3*). The total evaporation flux duration is $\tau_2 \approx 60$–70 ns. The time intervals of the processes are arranged in the sequence $\tau_2 > \tau_1 \gg \tau_0$, and the fullerite temperature determined by Eq. (1) is conventionally quasi-equilibrium.

Curve *4* in Fig. 4 illustrates the temperature conditions of formation of positively charged fullerenes. In this case, the working temperature range is 1600–1750 K, which is higher than the temperature range under the optimum conditions in Figs. 1 and 2 by 500–700 K. It is seen in Fig. 4 that the difference between the fullerite surface temperatures is 100–1300 K depending on the sign of charge of formed fullerenes and the delay time. The nature of the detected difference between the fullerite temperatures consists in the fact that, when a positively charged ion flux forms, the laser beam energy is consumed for fullerene evaporation and ionization (IE_i). However, when a fullerene flux forms under the action of a positive extracting voltage, an evaporated fullerene traps a π electron with affinity energy AE_i. Thus, as a result of ionization and affinity, a pair of fullerenes has different energies of formation,

$$\Delta E = AE_i + IE_i \le 2\varphi_\infty, \quad (4)$$

where $\varphi_\infty = 5.37$ eV is the work function of a graphite sheet [7]. The calculations performed for C_{20}–C_{150} fullerenes showed that $\Delta E = AE_i + IE_i = 10.6 \pm 0.2$ eV. As is seen from Eq. (4), the mass spectra of positively and negatively charged fullerenes differ substantially. During the formation of a negatively charged ion flux, the entire laser beam energy is consumed for heating of fullerites. Therefore, the surface temperature depends substantially on the sign of charge, and a temperature $T_{max} = 2950$ K is reached during the formation of a negatively charged ion flux.

4. OPTICAL PROPERTIES OF FULLERITE

According to the sublimation model generally accepted for the mixture fullerite [15], absorption layer L of laser radiation is determined with the following formula, which is similar to the Einstein equation for diffusion:

$$L = (2\varkappa\tau_1)^{0.5}, \quad (5)$$

where $\varkappa = \kappa/C_p\rho$ is the thermal diffusivity, κ is the heat-transfer coefficient, C_p is the specific heat of the fullerite, ρ is the material density, and τ_1 is the experimentally determined process time. The calculation of absorption layer thickness L is performed using the following data for the predominant component of the sample material, i.e., C_{60} fullerite: $\kappa = 0.4$ [7]; the specific heat of the material as a function of temperature is $C_p = 0.2 + 0.002T$, which was obtained by the extrapolation of the data for C_{60} fullerite [15]; and $\rho = 1.7 \times 10^3$ kg/m^3 [7, 15].

The substitution of numerical values into Eq. (5) shows that the absorption layer thickness is $L = 1.4 \times 10^{-6}$ m and the absorption coefficient of the fullerite is

$$k^* = 0.7 \times 10^6 \text{ m}^{-1}. \quad (6)$$

The calculation was performed using the AutoFlex (Bruker, Germany) data for an N_2 laser at a radiation power density $W = 0.33$ MW/cm^2.

CONCLUSIONS

(1) A temperature $T \le 1000$ K is achieved on the surface of the mixture fullerite subjected to laser irradiation at a radiation power density $W \le 0.1$ MW/cm^2, and sublimation predominantly takes place on this surface. At a pulsed laser radiation power density $W > 0.1$ MW/cm^2, the surface temperature is $T > 1000$ K, the destruction of the material on the surface is more intense, and secondary nanostructures (which were not detected in the initial material) form.

(2) The mass spectra of positively and negatively charged fullerenes differ in the nature of formation of the sign of cluster charge and in the energy of formation by $\Delta E = 10.6 \pm 0.2$ eV.

(3) The absorption coefficient of the fullerite for radiation at a wavelength $\lambda = 337$ nm at a radiation power density $W = 0.33$ MW/cm^2 is $k^* = 0.7 \times 10^6$ m^{-1}.

ACKNOWLEDGMENTS

We thank L.L. Fedorenko for useful discussions.

REFERENCES

1. V. F. Razumov, Nanotekhnol. Nauka Proizvod., No. 1 (6), 5 (2010).
2. D. G. Letenko, V. A. Nikitin, K. N. Semenov, N. A. Charykov, and A. S. Ivanov, Zh. Fiz. Khim. **86**, 1944 (2012).
3. F. Hillenkamp, M. Karas, R. C. Beavis, and B. T. Chait, Anal. Chem. **63**, 193 (1991).
4. M. M. Kasumov and O. I. V'yunov, Tech. Phys. **59** (2014) (in press).
5. A. M. Rao, Ping Zhou, Kai-An Wang, G. T. Hager, J. M. Holder, Ying Wang, W.-T. Lee, Xiang-Xin Bi, P. C. Eklund, D. S. Cornett, M. A. Duncan, and I. J. Amster, Science **259**, 955 (1993).
6. A. F. Shestakov, Ross. Khim. Zh. **51** (5), 121 (2007).
7. L. N. Sidorov, M. L. Yurovskaya, L. Ya. Borshchevskii, I. V. Trushkov, and I. N. Ioffe, *Fullerene* (Ekzamen, Moscow, 2005).
8. V. V. Dikii and G. Ya. Kabo, Usp. Khim. **69**, 107 (2000).
9. V. Piacente, G. Gigli, P. Scardala, A. Giustini, and D. Ferro, J. Phys. Chem. **99**, 114052 (1995).
10. V. Piacente, G. Gigli, P. Scardala, A. Giustini, and G. Bardi, J. Phys. Chem. **100**, 9815 (1996).
11. M. Nunez-Regueiro, L. Marques, J.-L. Hodeau, O. Bethoux, and M. Perroux, Phys. Rev. Lett. **74**, 2778 (1995).
12. V. V. Brazhkin and A. G. Lyapin, Phys. Usp. **39**, 837 (1996).
13. *Handbook of Physical Quantities,* Ed. by I. S. Grigor'ev and E. Z. Melikhov (CRC, Boca Raton, 1996).
14. M. M. Kasumov, L. V. Osaulenko, and V. V. Pokropivnyi, Ukr. Khim. Zh. **63** (12), 77 (2007).
15. V. D. Blank, A. A. Nuzhdin, V. M. Prokhorov, and R. Kh. Bagramov, Phys. Solid State **40**, 1261 (1998).

Translated by K. Shakhlevich

SPELL OK